Conformation-Dependent Cleavage of Hairpin and Triplex Nucleic Acids by a Temperature-Insensitive Photonuclease

Suzanne A. Ciftan and H. Holden Thorp*

Contribution from the Department of Chemistry, University of North Carolina at Chapel Hill, Chapel Hill, North Carolina 27599-3290

Received April 7, 1998

Abstract: Photolysis of $Pt_2(pop)_4^{4-}$ in the presence of duplex DNA produces strand scission via abstraction of the 4′- and 5′-hydrogen atoms (pop = $P_2O_5H_2^{2-}$). The cleavage intensities are higher for single-stranded DNA compared to those for duplex DNA because of lower electrostatic repulsion and greater solvent accessibility in single strands. When the single-stranded oligomer d(5′-ACTGCCTTTTTGCTGAA) was photolyzed in the presence of $Pt_2(pop)_4^{4-}$, there was no significant or systematic change in cleavage intensity as a function of temperature in the range 28 to 98 °C. Cleavage of the hairpin d(5′-ATCCTATTTTTTAGGAT) showed a higher cleavage intensity in the 5′-TTTTT loop region compared to that for the base-paired nucleotides. Thermal denaturation of the hairpin gave a less selective cleavage pattern. The increase in cleavage at the duplex nucleotides could be used to estimate the T_m for the folded hairpin; thus, the cleavage pattern reflects the thermal denaturation of individual nucleotides. This concept was tested on the oligomer d(5′-GAAGAG-GTTTTTCCTCTTCTTTTTCTTCTCC), which exists in either a single-, double-, or triple-stranded form, depending on the pH and temperature. The folded forms exhibit higher reactivity in the loop regions compared to that for the base-paired nucleotides. Thermal denaturation of the base-paired nucleotides could be distinguished in the cleavage patterns and correlated with conventional optical absorption data. While optical melting curves provide greater precision in the observed T_m values, the cleavage intensity approach allows mapping of multiple transitions to individual nucleotides in the sequence. The combination of both approaches therefore offers a powerful method for following thermal denaturation of DNA at A, T, and C nucleotides.

Introduction

The development of automated DNA synthesis,[1] PCR,[2] and SELEX[3] have necessitated a profusion of bioanalytical techniques for determining DNA structure and sequence. Understanding the role of secondary structure in the recognition and chemical reactions of nucleic acids would be expedited by simple methods for determining the secondary structure as a function of changes in the solvent environment or temperature.[4] In particular, the ability to visualize at every nucleotide changes in nucleic acid structure as a function of temperature would permit the assignment of secondary structure elements and their stabilities to individual regions of complex nucleic acids. Burrows and co-workers have discussed chemical reactions of divalent metal ions and persulfate that allow probing the conformation of guanine nucleotides as a function of temperature.[5] Herein we report a reaction that allows imaging of A, T, and C nucleotides.

The unusual photophysical and reactive properties of the d^8-d^8 dimer $Pt_2(pop)_4^{4-}$ (pop = $P_2O_5H_2^{2-}$)[6] are well suited to the study of nucleic acids.[7] Specifically, the long lifetime (10 μs) and intense phosphorescence emission (quantum yield, $\phi = 0.5$) characteristics[8] of $Pt_2(pop)_4^{4-}$ have provided for measuring DNA binding constants of weakly binding metal complexes.[9,10] In addition, $Pt_2(pop)_4^{4-*}$ abstracts the 4′- and 5′-hydrogen atoms from deoxyribose functions in duplex DNA.[11,12] This property was used to footprint the λ repressor protein binding sites by high-resolution gel electrophoresis.[13]

In addition to abstracting the 4′- and 5′-hydrogen atoms, the $Pt_2(pop)_4^{4-}$ excited state also oxidizes guanine by one-electron transfer;[14] however, sugar oxidation will be the focus of this study. The extent of sugar oxidation may be greatly enhanced using Mg^{2+}, which decreases the negative charge repulsion between the tetraanionic oxidant and the negatively charged polyanion and is useful for producing the even cleavage pattern needed for footprinting. In single-stranded DNA, there is much less electrostatic repulsion, and the sugar hydrogens are more solvent accessible. Single-stranded regions, therefore, exhibit greater reactivity than duplex DNA, especially at low concentra-

(1) Matteucci, M. D.; Caruthers, M. H. *J. Am. Chem. Soc.* **1981**, *103*, 3185.
(2) Saiki, R. K.; Gelfand, D. H.; Stoffel, S.; Scarf, S. J.; Higuchi, R.; Horn, G. T.; Mullis, K. B.; Erlich, H. A. *Science* **1988**, *239*, 487.
(3) Gold, L.; Tuerk, C. *Science* **1990**, *249*, 505−510.
(4) (a) Celander, D. W.; Cech, T. R. *Science* **1991**, *251*, 401−407. (b) Henderson, P. T.; Armitage, B.; Schuster, G. B. *Biochemistry* **1998**, *37*, 2991−3000. (c) Murakawa, G. J.; Chen, C. B.; Kuwabara, M. D.; Nierlich, D. P.; Sigman, D. S. *Nucleic Acids Res.* **1989**, *17*, 5361−5375.
(5) Muller, J. G.; Zheng, P.; Rokita, S. E.; Burrows, C. J. *J. Am. Chem. Soc.* **1996**, *118*, 2320−2325.
(6) Roundhill, D. M.; Gray, H. B.; Che, C.-M. *Acc. Chem. Res.* **1989**, *22*, 55−61.
(7) Carter, P. J.; Ciftan, S. A.; Sistare, M. F. *J. Chem. Educ.* **1997**, *74*, 641−645.
(8) Che, C.-M.; Butler, L. G.; Gray, H. B. *J. Am. Chem. Soc.* **1981**, *103*, 7796.
(9) Kalsbeck, W. A.; Thorp, H. H. *J. Am. Chem. Soc.* **1993**, *115*, 7146.
(10) Kalsbeck, W. A.; Thorp, H. H. *Inorg. Chem.* **1994**, *33*, 3427−3429.
(11) Kalsbeck, W. A.; Grover, N.; Thorp, H. H. *Angew. Chem., Int. Ed. Engl.* **1991**, *30*, 1517−1518.
(12) Kalsbeck, W. A.; Gingell, D. M.; Malinsky, J. E.; Thorp, H. H. *Inorg. Chem.* **1994**, *33*, 3313−3316.
(13) Briener, K. M.; Daugherty, M. A.; Oas, T. G.; Thorp, H. H. *J. Am. Chem. Soc.* **1995**, *117*, 11673−11679.
(14) Carter, P. J.; Briener, K.; Thorp, H. H. *Biochemistry* **1998**, *37*, 13736−13743.

S0002-7863(98)01166-4 CCC: $15.00
Published on Web 09/19/1998

tions of Mg^{2+} and other cations. Comparison of the relative cleavage intensities by electrophoresis allows discrimination between single-stranded and double-stranded regions.[14] In addition to the studies on secondary structure of guanine nucleotides mentioned above,[5] the discrimination of single-stranded regions is reminiscent of that observed by Schuster et al. with anthraquinones[4b] and for RNA by Sigman and co-workers with copper−phanthroline complexes.[4c] Herein we show that the secondary structure discrimination by $Pt_2(pop)_4^{4-}$ is independent of temperature, so that thermal denaturation of individual nucleotides can be followed from the cleavage yields. Application of this approach to DNA hairpins and triplexes is described.

Experimental Section

Materials. Oligodeoxynucleotides were purchased from the Oligonucleotide Synthesis Center of the UNC−CH Department of Pathology and purified by gel cutting. The single-stranded sequences were annealed by heating at 90 °C for 5 min in the appropriate buffer and immediately cooled in an ice/water bath. 5′-[^{32}P]-labeled oligonucleotides were prepared from 5′-[γ-^{32}P]-dATP (Amersham) and T4 polynucleotide kinase (New England Biolabs). The metal complex $Pt_2(pop)_4^{4-}$ was prepared by the literature method.[15] All of the reagents were used without further purification.

DNA Oxidation. The 20-μL reaction volume consisted of the 5′-[^{32}P]-labeled oligodeoxynucleotide, 2 mM Tris-HCl buffer at the appropriate pH, $Pt_2(pop)_4^{4-}$, and 0.5 μg of calf thymus DNA. In addition, 25 mM NaCl and 3 μM $MgSO_4$ were used for the DNA triplex reaction. Reactions were photolyzed for 5 min with an Oriel 68810 arc Hg lamp at 300 W and a 368-nm wavelength in 100-μL glass polyspring insert (Fisher). Reaction temperatures were controlled in a polyspring insert placed into a 1-cm path length quartz cell encased by a UV/vis spectrophotometer thermal jacket. The temperature of the reaction was controlled by a Fisher Isotemp model 900 refrigerated ethylene glycol/water circulator and was measured using a Physitemp type IT-18 thermocouple and a Baxter S/P digital thermometer. Removal of Pt-bound DNA required incubation with 10 μL of 1 M KCN and 2 μg of calf thymus DNA at 50 °C for 30 min, followed by ethanol precipitation.[13] All of the DNA reactions were treated with 60 μL of 0.7 M piperidine at 90 °C for 30 min.

The cleavage band intensities were measured by scanning the Kodak Biomax MR X-ray film using a Macintosh OneScanner equipped with Ofoto 2.0 and were integrated using the NIH Image 52 software. Care was taken to ensure that saturation of the film did not occur. To generate the temperature plots, the raw intensities were normalized to the most intense loop residue in each lane, which was always the same residue on each gel. The normalized intensities for the group of nucleotides being analyzed (i.e., T5 + T12 or T9 − T11 in Figure 1 and the TS or DS nucleotides for Figures 2−4) were then summed. These summed intensities were then placed on a relative intensity scale (from 0 to 1) as (intensity − $\text{intensity}_{\text{initial}}$)/($\text{intensity}_{\text{final}}$ − $\text{intensity}_{\text{initial}}$). For the loop residues shown as a control in Figure 1 (T9−T11), the final intensity for the T5 + T12 group was used as $\text{intensity}_{\text{final}}$ so that the two groups could be displayed on the same scale and the precision could be assessed. The average of the intensities of the TS and DS nucleotides shown in Figure 3C and Figure 4C is simply the mathematical average of the two relative intensity values from Figures 3B and 4B; both of the TS and DS sets contain the same number of nucleotides.

Ultraviolet Thermal Denaturation. Ultraviolet thermal denaturation curves were obtained by monitoring the oligodeoxynucleotide absorption at 260 nm as a function of temperature. The 1-mL solution sample was measured with a Hewlett-Packard UV−vis diode array spectrophotometer in a 1-cm path length quartz cell equipped with a thermal jacket and a Fisher Isotemp model 900 refrigerated ethylene glycol/water circulator. The temperature was measured using a Physitemp type IT-18 thermocouple and a Baxter S/P digital thermometer. Data were plotted using Kaleidagraph software, and the average of the pre- and postdenaturation absorption was used to determine the melting temperature. UV thermal denaturation experiments were run under the same conditions as the photolysis experiments, except that $Pt_2(pop)_4^{4-}$ was absent.

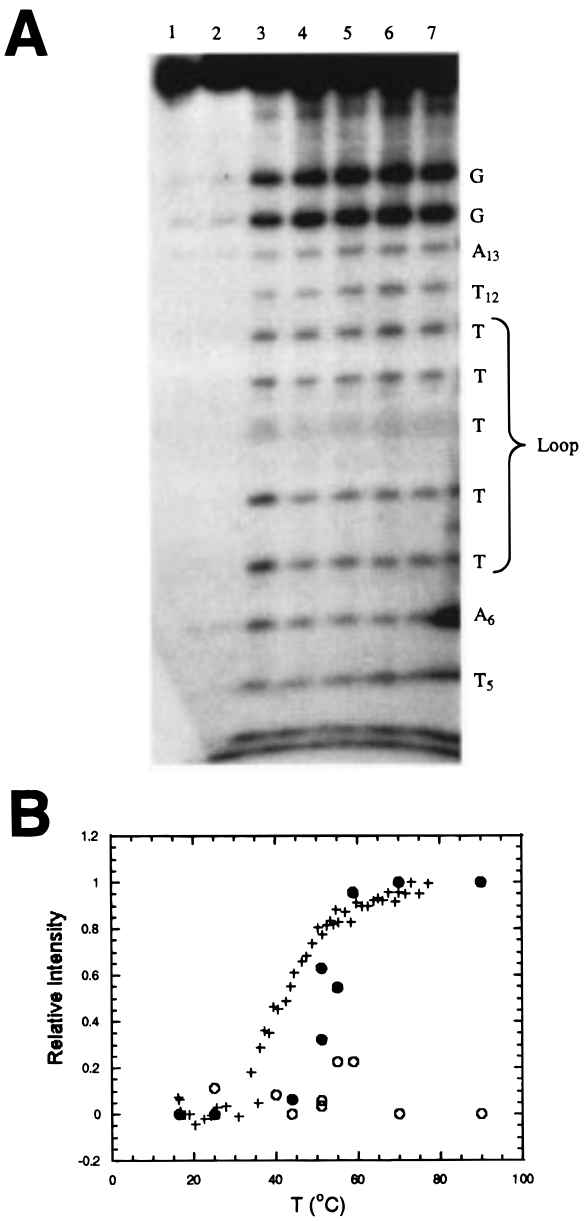

Figure 1. (A) Autoradiogram of the 20% polyacrylamide sequencing gel for the d(5′-ATCCTATTTTTTAGGAT) hairpin as a function of temperature in 2 mM Tris-HCl buffer (pH 7) and 0.5 μg calf thymus DNA. Lane 1: Maxam−Gilbert G lane; lane 2: DNA control; lanes 3−7: 150 μM $Pt_2(pop)_4^{4-}$ at 25 °C, 44 °C, 51 °C, 56 °C, and 58 °C, respectively. (B) Plot of the cleavage intensity for the average of two different stem nucleotides (●, T5 and T12) and three loop residues (○, T9 − T11) as a function of temperature. Data from lane 7 of Figure 1A were not used because of contamination from an adjacent lane. Cleavage intensities were averages from two different gels and were normalized as described in the Experimental Section. Also shown is the UV absorption curve (+) measured in the same buffer as that for the cleavage yield.

Results

Hairpin Oxidation. Since our goal was to develop a photocleavage reaction where the temperature dependence could be interpreted in terms of conformational changes in the nucleic

(15) Che, C.-M.; Butler, L. G.; Grunthaner, P. J.; Gray, H. B. *Inorg. Chem.* **1985**, *24*, 4662−4665.

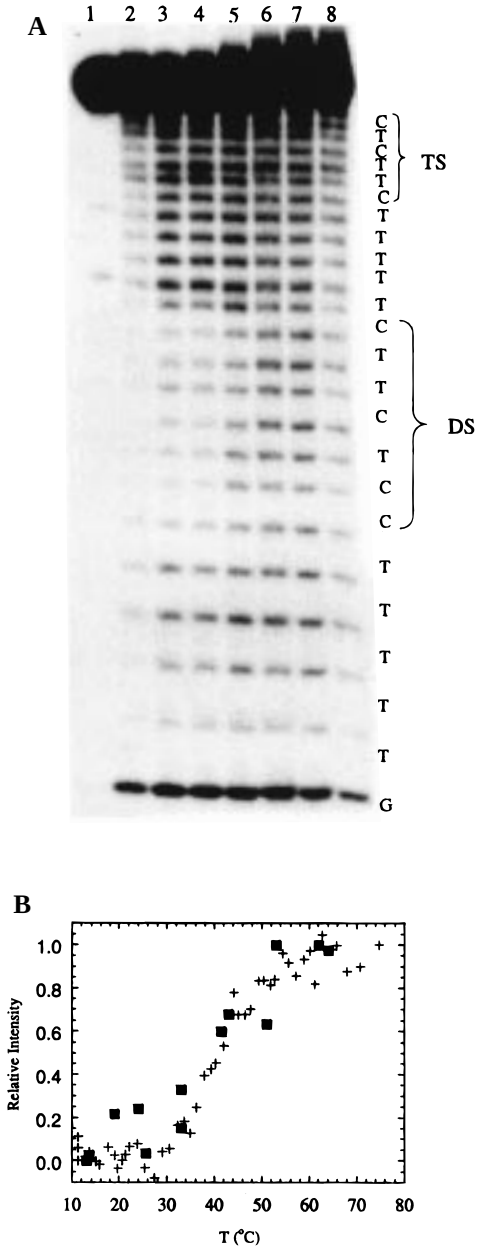

Figure 2. (A) Autoradiogram of the 20% polyacrylamide sequencing gel for the reaction of $Pt_2(pop)_4^{4-}$ (pH 7.4) and the d(5′-GAAGAG-GTTTTTCCTCTTCTTTTTCTTCTCC) triplex with increasing temperature. The central segment that forms the duplex (5′-CCTCTTC) is referred to as DS, and the segment that completes the triplex (5′CTTCTCC) is referred to as TS. The folded oligomer exhibits a single thermal transition in 2 mM Tris-HCl buffer (pH 7.4), 25 mM NaCl, 7 μM $MgCl_2$, and 0.3 μM calf thymus DNA. Lane 1: DNA control; lanes 2−8: 95 μM $Pt_2(pop)_4^{4-}$ at 13 °C, 24 °C, 33 °C, 43 °C, 53 °C, 64 °C, and 73 °C, respectively. (B) Plot of the cleavage intensity for the DS region (■) and the UV absorption (+) as a function of temperature.

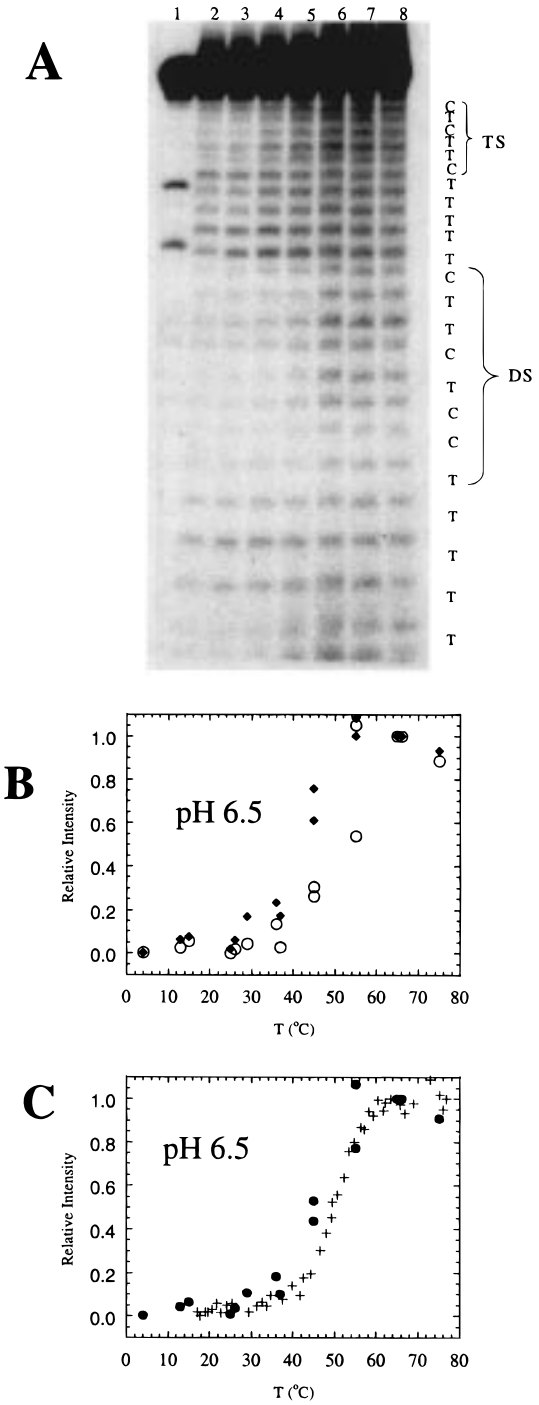

Figure 3. (A) Autoradiogram of the 20% polyacrylamide sequencing gel for the reaction at pH 6.5 of the d(5′-GAAGAGGTTTTTCCTCT-TCTTTTTCTTCTCC) triplex and $Pt_2(pop)_4^{4-}$ with increasing temperature. The TS segment denatures before the DS segment in 2 mM Tris-HCl buffer (pH 6.5), 25 mM NaCl, 7 μM $MgCl_2$, and 0.3 μM calf thymus DNA. Lane 1: DNA control; lanes 2−8: 150 μM $Pt_2(pop)_4^{4-}$ at 13 °C, 26 °C, 36 °C, 45 °C, 55 °C, 65 °C, and 75 °C, respectively. (B) Plot of the cleavage intensity as a function of temperature for the TS (◆) and DS (○) nucleotides. (C) Plot of the average cleavage intensity for the TS and DS regions (●) and the UV absorption (+) as a function of temperature.

acid, we first sought to investigate as a control a nucleic acid that did not exhibit a temperature-dependent structural change. The $Pt_2(pop)_4^{4-}$ complex was photolyzed with the single-stranded DNA sequence d(ACTGCCTTTTTGCTGAA) at temperatures between 25 and 65 °C. No significant or systematic changes in the cleavage intensities within the sequence were observed across the temperature range (intensity plots shown in Supporting Information). This result suggests that if significant and systematic changes in the cleavage pattern were obtained with different sequences, then these could be ascribed to conformational changes in the nucleic acid rather than to an effect of temperature on the intrinsic photocleavage reaction.

We next sought to demonstrate that the photoreaction of an oligonucleotide with a well-characterized structural transition exhibited a predictable temperature profile. The DNA hairpin d[5′- ATCCTATTTTTTAGGAT] is known to undergo melting

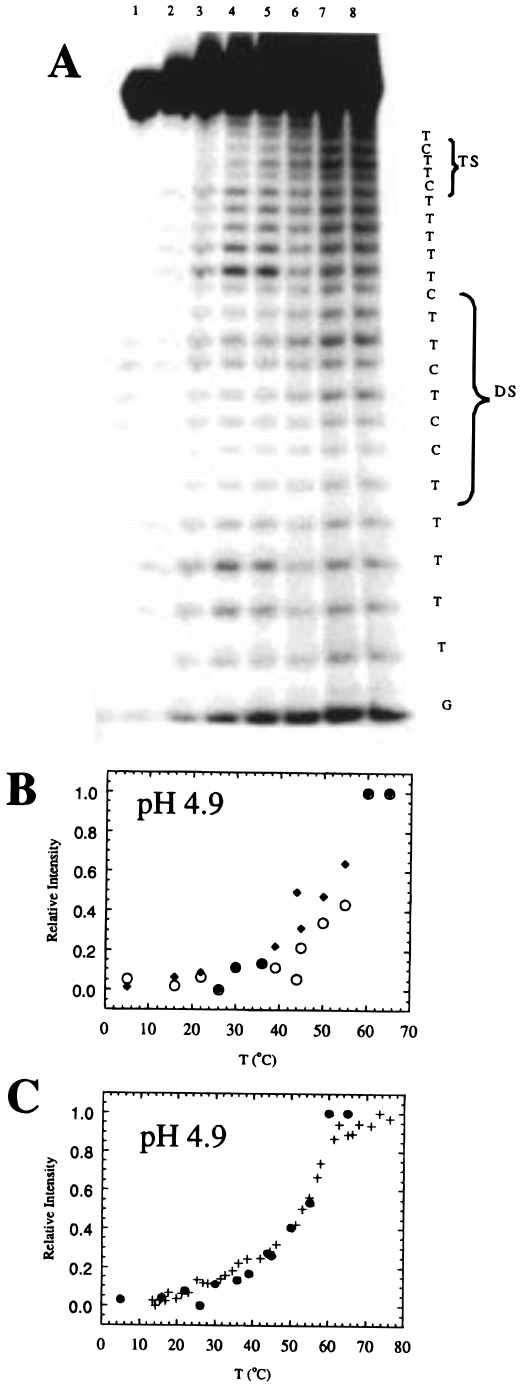

Figure 4. (A) Autoradiogram of the 20% polyacrylamide sequencing gel for the reaction of $Pt_2(pop)_4^{4-}$ at pH 4.9 for the d(5′-GAAGAG-GTTTTTCCTCTTCTTTTTCTTCTCC) triplex with increasing temperature. The folded oligomer exhibits one transition to the single-stranded form in 2 mM Tris-HCl buffer (pH 4.9), 25 mM NaCl, 7 μM $MgCl_2$, and 0.3 μM calf thymus DNA. Lane 1: DNA control; lanes 2−8: 95 μM $Pt_2(pop)_4^{4-}$ at 15 °C, 26 °C, 36 °C, 45 °C, 55 °C, 65 °C, and 76 °C, respectively. (B) Plot of the cleavage intensity as a function of temperature for the TS (◆) and the DS (○) nucleotides. (C) Plot of the average cleavage intensity for the TS and DS regions (●) and the UV absorption (+) as a function of temperature.

to the single-stranded form at 51 °C.[16] As we have discussed elsewhere, single-stranded regions of hairpins are oxidized to a greater extent than adjacent double-stranded regions because of greater solvent accessibility and lower electrostatic repulsion of the tetraanionic $Pt_2(pop)_4^{4-}$ complex. Accordingly, cleavage of the folded hairpin at room temperature showed the greatest cleavage in the 5′-TTTTT loop region (lane 3, Figure 1A). The intensities at guanines are greater than at other nucleotides because of a side reaction involving electron transfer to $Pt_2(pop)_4^{4-}$*, as we have discussed in detail elsewhere.[14] Lower concentrations of $Pt_2(pop)_4^{4-}$ were used to obtain the optimum selectivity for the single-stranded region of the folded hairpin.

The DNA hairpin stability was measured by varying the temperature during the photolysis. As shown in Figure 1A, the intensity of cleavage throughout the hairpin becomes more equivalent at each nucleotide as the temperature is raised. The cleavage intensities of stem nucleotides, determined from two experiments, are plotted as a function of temperature in Figure 1B. The temperature profile exhibits a sigmoidal temperature dependence typical for hairpin denaturation. The melting temperature (T_m) determined from the inflection point was within 5 °C of the known melting temperature of 51 °C.[16] The temperature dependence of the reaction can therefore be ascribed to the known conformational change. As discussed in more detail below, the differences of 5−10 °C in the optical and cleavage T_m's are due to experimental error in the cleavage method and precise T_m's are advantageously obtained using absorption. The thermal transition for the hairpin from Figure 1 was observed by optical absorption under the same buffer conditions, and the data are also plotted in Figure 1B. Intensities for the loop residues T9, T10, and T11 are also plotted in Figure 1B to show that there is no significant or systematic effect of temperature on the loop region.

Triplex Oxidation. There is considerable interest in the structure and stability of triplexes given their importance in fundamental biochemistry, diagnostics, and antisense therapeutics.[17−19] DNA triple helices that fold intramolecularly allow for observation of triple-, double-, and single-stranded forms within one oligomer and are particularly useful for NMR and thermodynamic studies where bimolecular reactions are undesirable.[20−22] In addition to being studied with NMR, triplexes have been studied using S1 nuclease[23] and X-ray crystallography.[24] The 31-mer in Scheme 1 has three segments that fold back to form a pyr·pur·pyr motif.[25] The double-stranded region exhibits Watson−Crick base pairing, and the third strand forms Hoogsteen base pairs, which are formed with the duplex strand in the major groove. The Hoogsteen base pairs may be thermally disrupted selectively to form a hairpin consisting of a pyr·pur duplex a 3′-tail. Further unfolding of the duplex to the single-stranded coil then occurs at higher temperature. This behavior is very sensitive to the pH and buffer conditions.

The melting behavior of this triplex in pyrophosphate buffer was studied by Plum and Breslauer using calorimetry and spectroscopy.[25] Circular dichroism spectra were taken in each temperature regime before and after each melting transition to confirm the presence of the single-stranded, duplex, and triplex forms at each pH. At pH 8, the only two stable forms are the duplex and single strand, while at pH 6.5, two thermal transitions

(16) Hilbers, C. W. *Biochimie* **1985**, *67*, 685.
(17) Pascolo, E.; Toulmé, J.-J. *J. Biol. Chem.* **1996**, *271*, 24187−24192.
(18) Svinarchuk, F.; Paoletti, J.; Malvy, C. *Nucleic Acids Res.* **1995**, *270*, 14068−14071.
(19) Hanvey, J. C.; Klysik, J.; Wells, R. D. *J. Biol. Chem.* **1988**, *263*, 7386−7396.
(20) Koshlap, K. M.; Shultze, P.; Brunar, H.; Dervan, P. B.; Feigon, J. *Biochemistry* **1997**, *36*, 2659−2668.
(21) Radhakrishnan, I.; Patel, D. *J. Am. Chem. Soc.* **1991**, *113*, 8542−8544.
(22) Sklenár, V.; Feigon, J. *Nature* **1990**, *345*, 836−838.
(23) Johnston, B. H. *Science* **1988**, *241*, 1800−1804.
(24) Vlieghe, D.; Meervelt, L. V.; Dautant, A.; Gallois, B.; Précigoux, F.; Kennard, O. *Science* **1996**, *273*, 1702−1705.
(25) Plum, G. E.; Breslauer, K. J. *J. Mol. Biol.* **1995**, *248*, 679−695.

Scheme 1

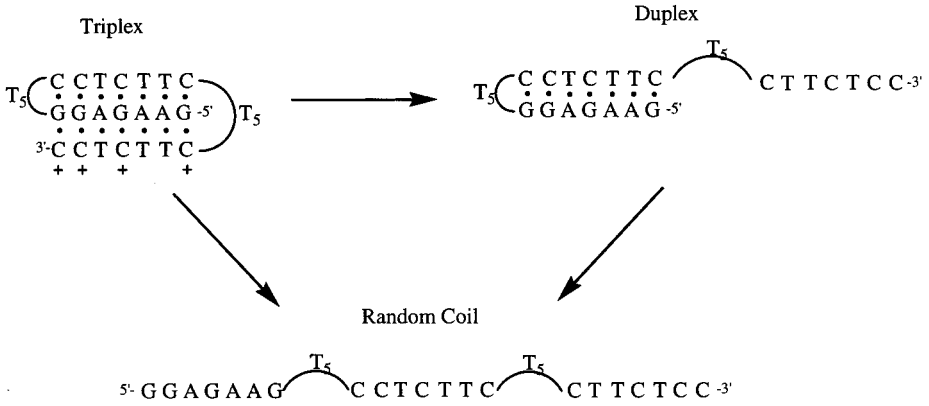

were observed that convert the triplex to the duplex and then to the single strand. At pH 5.0, the triplex melts cooperatively to the single-stranded coil form without a duplex intermediate.[25] These observations were confirmed in our hands by optical absorption in pyrophosphate buffer, and results identical to those of Plum and Breslauer were obtained (data given in Supporting Information). In the pyrophosphate buffer used by Plum and Breslauer,[25] we found that the photochemistry of $Pt_2(pop)_4^{4-}$ was quenched; therefore, we performed the photocleavage experiments in Tris buffer. The change in buffer conditions altered the stability of the three states, which was then confirmed independently by optical absorption as described below.

The cleavage patterns obtained upon photolysis of $Pt_2(pop)_4^{4-}$ were determined for the triplex oligonucleotide at pH 7.4 (Figure 2), pH 6.5 (Figure 3), and pH 4.9 (Figure 4). Photoreactions of the oligonucleotide under conditions where the DNA triplex is stable at room temperature (pH 4.9 and 6.5) showed greater cleavage in the loop regions, as shown in lane 3 of Figures 3A and 4A. This result is similar to that of the DNA hairpin oligomer, where the single-stranded loop regions are easily identified by an increase in cleavage. The results also allow us to assess the reactivity of the photooxidant toward both the double- and triple-stranded segments. The intensities for the triplex-forming bases (5′-CTTCTCC; TS) and the duplex-forming bases (5′-CCTCTTC; DS) are approximately equal in the folded state, suggesting that the accessibility of both regions toward $Pt_2(pop)_4^{4-}$ are nearly equivalent.

The photooxidation reaction was performed on the duplex structure at pH 7.4. At this pH, the oligomer is partially unfolded and comprises a duplex segment with a single-stranded coil of sequence 5′-TTTTTCTTCTCC, derived from the 3′-loop and the TS segment. This single-stranded coil is readily observed by inspection of the room-temperature reaction from the autoradiogram in lane 3 of Figure 2A, which shows a large and similar extent of oxidation for all of the nucleotides in the 3′-loop and the TS segment. In addition, the 5′-loop is more reactive than the duplex segments although not as reactive as the single-stranded tail. These results are consistent with the structure of a hairpin and a 3′ tail. The extent of the photooxidation reaction from 13 to 73 °C at pH 7.4 is shown in Figure 2B. In this case, the double- to single-stranded transition is apparent as an increase of the extent of oxidation of the DS nucleotides from 33 to 64 °C. The extent of oxidation is nearly equivalent for all nucleotides at 64 °C, which suggests that the oligomer is fully denatured.

As with that of the single hairpin, the melting temperature may be assessed from a plot of the cleavage intensity at the duplex nucleotides as a function of temperature. For all thermal denaturation plots, the average intensity for all bases within the segment of interest was plotted as a function of temperature and utilized at least two data sets obtained from independent experiments. The plot in Figure 2B shows the cleavage intensity of the double-stranded region as a function of temperature at pH 7.4. The T_m determined from either the inflection point of a curve that fits the data points or from the temperature at which the average cleavage intensity is achieved was 42 °C, which was lower than that observed with optical absorption by Plum and Breslauer using pyrophosphate buffer at the same pH and salt conditions.[25] In our buffer, we observed a melting temperature by optical absorption of 42 °C, which agreed well with that obtained from the cleavage data. Figure 2B shows the results of both the photooxidation and the UV thermal denaturation in Tris-HCl on the same graph. In addition to supporting the ability of the photooxidation to assess the appropriate melting temperature and number of thermal transitions, these results support a less stable duplex in Tris-HCl compared to pyrophosphate buffer.

The photooxidation reaction may be used to separate two overlapping melting transitions that occur at different nucleotides. For example, Plum and Breslauer observed two transitions at pH 6.5 that were resolvable by optical absorption.[25] In Tris-HCl buffer, we could not resolve these two transitions by absorbance. Figure 3A displays the results of the photocleavage reaction at pH 6.5 with increasing reaction temperatures. The TS cleavage intensity increases from 36 to 55 °C, whereas the intensity for the DS segment starts increasing at 55 °C. The plot in Figure 3B shows the resolution of these two melting transitions when the triple- and double-stranded segments are plotted separately. The T_m for the TS and DS segments are 45 and 55 °C, respectively. We suspected that the absorbance curve failed to resolve the two transitions because the average degree of single-strandedness was assessed for the entire oligonucleotide. Accordingly, a plot of the average of the intensities for the triple- and double-strands gave a curve very similar to that obtained from the absorbance data (Figure 3C).

At pH 4.9, the triplex is completely folded at room temperature, and by absorbance is observed upon heating to unfold from the triplex directly to the coil without a double-stranded intermediate.[25] The extent of oxidation for the double- and triple-stranded segments can be followed as a function of temperature in the autoradiogram of Figure 4A. As the temperature increases, the onset of the increase in the intensity of the DS segment occurs at nearly the same temperature as the increase in the intensity of the TS segment. This result supports the absence of an intermediate duplex structure; the data are plotted in Figure 4B. The relative intensity is equivalent for the triple- and double-stranded regions between 25 and 36

°C. The UV absorption data again match well with average of the triplex and duplex photooxidation yields (Figure 4C).

Discussion

A difficult challenge in the development of chemical nucleases is to engineer the oxidation chemistry such that changes in the cleavage pattern can be confidently assigned to perturbations in the biomolecule structure rather than to changes in the oxidation chemistry.[4,5,26,27] Likewise, the oxidation chemistry should ideally allow for a wide range of buffer, metal cation, pH, and temperature conditions.[28] Photonucleases activated by visible light are attractive from this point of view because biological buffers are unlikely to be photoreactive and biomolecules are generally only photoreactive in the UV region. As we show here for example, pyrophosphate quenches the photochemistry of $Pt_2(pop)_4$,$^{4-}$ and chemical reactions between the buffer and nuclease are an important constraint in this and any other system. The requirement, however, that the cleavage chemistry be independent of temperature is a challenging one for photonucleases because of the effects of temperature on many photophysical and photochemical properties.[29] As discussed elsewhere, the photophysics of $Pt_2(pop)_4^{4-}$ are quite insensitive to both temperature and solvent compared to those of many other inorganic excited states.[6] As described here, the photocleavage chemistry of $Pt_2(pop)_4^{4-}$ is sufficiently insensitive to temperature so that changes in the cleavage pattern can be ascribed to changes in the biomolecule structure.

One drawback to the present system is that guanine nucleotides undergo reaction by a separate one-electron pathway that is less sensitive to solvent accessibility.[14] In the cases described here, the guanines do not dominate the chemistry to an extent that precludes analysis of the other three nucleotides. This case will not obtain with RNA, because the 2′-hydroxyl deactivates sugar hydrogens that are abstracted by $Pt_2(pop)_4^{4-}$*,[30] which causes the guanine oxidation to dominate the cleavage pattern completely.[14] Thus, our analysis is limited to A, T, and C nucleotides in DNA.

The photocleavage pattern of $Pt_2(pop)_4^{4-}$ did not show systematic or significant changes in the cleavage pattern with a single-stranded oligomer as a function of temperature, and studies of a simple DNA hairpin gave a melting temperature for the hairpin within experimental error of that measured by optical absorption. The changes in the cleavage pattern do not give melting temperatures with precision equaling that of those obtained by spectroscopy; however, the temperature-dependent cleavage pattern provides a means for mapping the thermal transitions to individual nucleotides in the sequence. Furthermore, the precision in the transition temperatures observed by photocleavage is sufficient to allow correlation with the transitions observed by absorption so that the combination of the two approaches should be particularly powerful.

The triplex-forming sequence developed by Plum and Breslauer[25] offers an excellent forum for testing our approach. The sequence can exist in three different states, which can be thermally interconverted depending on the pH. In particular, we have shown that the cleavage at the duplex- and triplex-forming nucleotides increases upon denaturation and that these changes occur at the temperatures expected from the optical absorption profiles. Further, the average of the cleavage intensities for the DS and TS nucleotides reproduces the optical absorption curves with good agreement.

The results on the fully folded triplex show that the chemical reactivity of $Pt_2(pop)_4^{4-}$ toward the triplex and duplex strands is very similar. We have shown previously that the complex abstracts the 4′- and 5′-hydrogens in duplex DNA largely on the basis of the solvent accessibility of these hydrogens. We have not determined the chemical mechanism for strand scission in the single-stranded and triplex forms; therefore, the greater reactivity in the single-stranded regions may result either from greater solvent accessibility for the 4′- and 5′-hydrogens or from additional reaction pathways involving other deoxyribose hydrogens that are available in the single-stranded regions. In either event, the greater reactivity of the single-stranded regions can be used to map thermally induced structural changes to individual nucleotides in the structure.

Acknowledgment. This work was supported by the National Science Foundation. H.H.T. acknowledges the support of a Camille Dreyfus Teacher-Scholar Award and an Alfred P. Sloan Fellowship.

Supporting Information Available: Plots of cleavage intensity and absorbance as a function of temperature (2 pages, print/PDF). See any current masthead page for ordering information and Web access instructions.

JA981166R

(26) Thorp, H. H. *Adv. Inorg. Chem.* **1995**, *43*, 127−177.
(27) Tullius, T. D.; Dombroski, B. A. *Proc. Natl. Acad. Sci. U.S.A.* **1986**, *83*, 5469−5473.
(28) Theil, E. C. *New J. Chem.* **1994**, *18*, 435−441.
(29) Turro, N. J. *Modern Molecular Photochemistry*; Benjamin-Cummings: Menlo Park, CA, 1978.
(30) Neyhart, G. A.; Cheng, C.-C.; Thorp, H. H. *J. Am. Chem. Soc.* **1995**, *117*, 1463−1471.